

## Luminescence Quenching in Magnesium-Doped Alumina Ceramics

S. V. Zvonarev<sup>a,\*</sup> and N. O. Smirnov<sup>a</sup>

<sup>a</sup> Ural Federal University Named after the First President of Russia B.N. Yeltsin, Yekaterinburg, Russia

\*e-mail: s.v.zvonarev@urfu.ru

Received December 4, 2018; accepted December 5, 2018

**Abstract**—The effect of magnesium impurity on luminescent properties of alumina ceramics sintered at high temperatures under vacuum is studied by pulsed cathodoluminescence, photoluminescence, and thermoluminescence. At dopant concentrations  $>1$  wt %, high-temperature synthesis results in formation of defects associated with magnesium, which were identified in the pulsed cathodoluminescence (520 nm) and photoluminescence (767 nm) spectra, as well as in the thermoluminescence curves (380 K). It is found that increased magnesium concentration leads to luminescence quenching of the intrinsic centers ( $F$  centers) of alumina in the PCL emission band at 400 nm, impurity defects ( $Mn^{4+}$  and  $Cr^{3+}$ ) in the photoluminescence emission bands at 673 and 689 nm, and all the recorded thermoluminescence peaks at 380, 450, and 615 K.

DOI: 10.1134/S1063783419050408

### INTRODUCTION

Luminescent properties of materials are being intensively studied in order to design highly efficient luminophores based on these materials. Among those materials, oxide systems used in various fields of research and engineering are of keen interest [1–3]. Monocrystalline and nanostructured alumina is currently employed as a sensor for luminescence dosimetry of ionizing radiation [4, 5]. The luminescent properties of this material depend on its structural state and charge-transfer mechanisms. It is particularly interesting to study these processes if the material contains different defects that can capture free charge carriers [6]. Changes in their population density result in redistribution of probabilities of competing processes of electron and hole transfer between the defect centers and delocalized zones, thus altering the luminescent properties of the material. Experimental research into the optical properties of these faulty materials is of significant interest for understanding the features of the structural state of novel functional materials and for predicting their properties.

Luminescent properties are changed due to formation of impurity defects as the initial alumina matrix is doped with various transition metal ions (e.g., chromium [7], manganese [8], magnesium, and titanium [9]). Alumina is most commonly used as the initial oxide matrix. High luminescence intensity at a certain wavelength in this material can also be achieved by doping with such rare earth metals as europium [10], erbium [1], neodymium [12], and terbium [13]. Structural defects (oxygen vacancies and impurities centers in particular) play a key role in binary and multicomponent oxides, including alumina [14, 15].

In many cases, magnesium is used as an impurity in the initial alumina matrix for creating the anion defect structure [16, 17]. Magnesium aluminate spinel with various impurities is currently being studied as the initial matrix that can potentially be used in optics [18–20]. Special focus is placed on induced defects contributing to the emergence of luminescence in these ceramics [21]. The intensity of intrinsic luminescence bands of the matrix, the impurity centers (and potentially the newly formed aggregate and cluster centers) is expected to largely depend on impurity concentration and the related mechanisms of concentration quenching and competing effects. Hence, this study focused on luminescent properties of the magnesium-doped alumina ceramics depending on impurity concentration using pulsed cathodoluminescence (PCL), photoluminescence (PL), and thermoluminescence (TL).

### EXPERIMENTAL

Magnesium-doped alumina ceramics were fabricated by high-temperature sintering of the compacts preimpregnated with magnesium nitrate solution. The ceramics were sintered under vacuum at  $P = 0.013$  Pa on an SNVE 9/18 high-temperature vacuum electric furnace for 2 h at temperature varied from 1500 to 1700°C. Doping was performed by impregnating the initial compact with magnesium nitrate (impurity concentration was varied from 0.01 to 6.85 wt %). The maximum impurity concentration that could be reached using this doping method was limited by formation of a saturated solution of this salt at room temperature. The impregnation duration was chosen to be 1 h as it ensured uniform distribution of the impurity

over the entire sample volume. The initial compacts were fabricated by cold isostatic pressing of  $\alpha$ - $\text{Al}_2\text{O}_3$  powder on a PRG-1-50 hydraulic press at  $P = 0.7$  GPa. The commercial nanopowder with grain size of 10–150 nm was synthesized using the alcoholate method. Before impregnation, the samples were annealed at 450°C for 2 h to enhance their mechanical strength. In order to obtain a series of ceramic samples characterized by high concentration of intrinsic defects, some of the samples were stained thermochemically during sintering under vacuum in the presence of carbon using high-purity graphite rods (20 g). Carbon is a good reducing medium and allows one to obtain oxygen-deficient ceramics. Details of the method used to prepare the samples were presented in [22].

Charge transfer and the effect of nonstoichiometry on luminescent properties of the resulting ceramics, which are caused by the presence of defects and impurity centers, were studied experimentally using a combination of methods of pulsed cathodoluminescence, photoluminescence, and thermoluminescence. The cathodoluminescence spectra were recorded on a KLAVI spectrometer (with a pulse duration of 2 ns, average electron energy of  $130 \pm 10$  keV, current density of 60 A/cm<sup>2</sup>, pulse frequency of 1 Hz, and the spectral range of 350–750 nm). Photoluminescence was measured on an LS-55 spectrometer (Perkin Elmer) with a pulsed xenon lamp used as a source of light; the range of excitation and emission was 200–515 nm and 430–900 nm, respectively. The measurements were made in the phosphorescence mode with the delay time of 0.02 ms. Spectra in the fluorescence mode could not be recorded, because of an intense glow of the sample. TL was measured for an experimental sample of the Gray dosimetric system at linear heating in the temperature range of 300–670 K at a heating rate of 2 K/s using an H10722 photomultiplier (HAMAMATSU Photonics, Japan). TL was excited using an electron beam gun (1.5 kGy per pulse).

## RESULTS AND DISCUSSION

High-temperature synthesis of magnesium-doped alumina ceramics gives rise both to intrinsic defects of the matrix and impurity centers (Fig. 1). The emission band with the maximum at 400 nm corresponds to luminescence of the  $F$  center of alumina [14]. This center is an oxygen vacancy with two electrons captured in it. The most intense band in the PCL spectrum is associated with the  $R$ -band of chromium (693 nm) [23], which could be present in the initial powder at low concentrations. At high concentrations of magnesium ions, the spectrum contains an emission band at 520 nm corresponding to the aggregate center  $F_2^{2+}$  (2Mg) that was formed during synthesis [24]. In a number of studies, this band was found to be associated with the aggregate  $F_2$  centers formed by

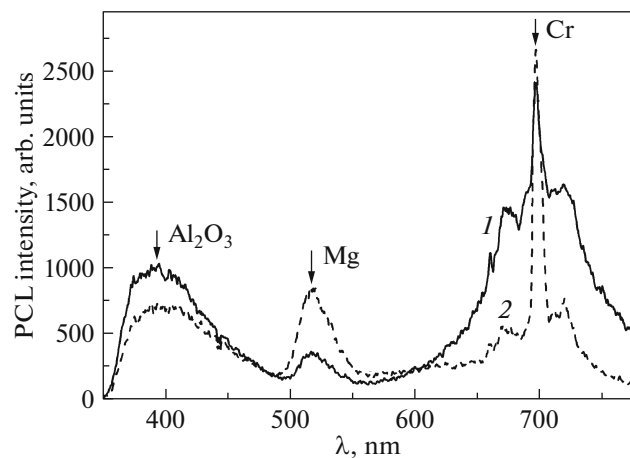


**Fig. 1.** PCL spectra of the  $\text{Al}_2\text{O}_3:\text{Mg}$  ceramics sintered at 1500°C under vacuum: (1) in the presence and (2) in the absence of carbon.

oxygen vacancies and the centers formed by aluminum ions [21]. It is known from the literature data [25] that high-temperature sintering in the presence of carbon facilitates formation of  $F$  centers. Carbon becomes gaseous at a sintering temperature above 1500°C. It is chemically reactive and interacts with oxygen of the initial alumina matrix. This results in oxygen nonstoichiometry, and the ceramics becomes oxygen-deficient. This regularity was also confirmed for the ceramics under study. Luminescence intensity at 400 nm is higher for the samples sintered in the presence of carbon. It should be mentioned that the intensity of the emission band at 520 nm decreases. In this connection, it is fair to say that it is impurity centers of magnesium rather than the aggregate centers formed by oxygen vacancies that make the main contribution to luminescence at 520 nm.

As demonstrated in the previous studies [26], the concentration of  $F$  centers rises with increasing sintering temperature for the impurity-free ceramics. The same effect is observed for the magnesium-doped alumina ceramics. Thus, luminescence intensity at 400 nm for the ceramics sintered at 1700°C (Fig. 2, curve 3) is higher than that for the ceramics sintered at 1500°C (Fig. 1, curve 2) by almost 1.5-fold. The increased sintering temperature also enhances the luminescence intensity at 520 nm. More impurity centers are formed at high temperature as magnesium replaces aluminum ions and magnesium ions are embedded at the interstitial sites, thus forming magnesium spinel. This effect is not observed at low impurity concentrations. Figure 2 shows the CPL spectra of the  $\text{Al}_2\text{O}_3:\text{Mg}$  ceramics sintered at 1700°C during 2 h as dopant concentration was varied. We found that the emission band at 520 nm is recorded only at the maximum concentration of impurity in the ceramics. The

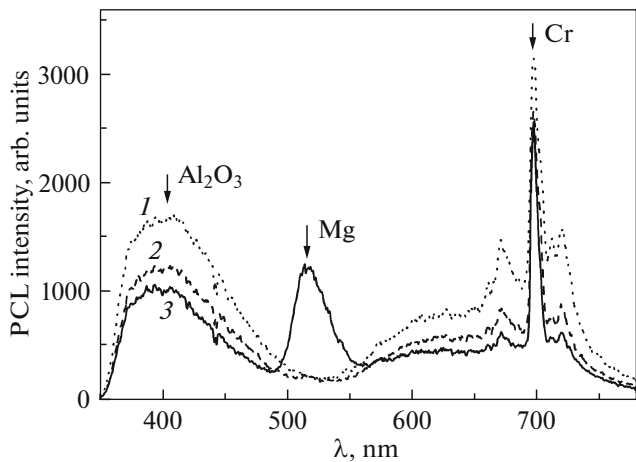


**Fig. 2.** PCL spectra of the  $\text{Al}_2\text{O}_3:\text{Mg}$  ceramics sintered at  $1700^\circ\text{C}$  at different concentrations: (1) 0.1; (2) 1; and (3) 6.85 wt %.

increasing magnesium concentration leads to luminescence quenching in the emission band of  $F$  center.

The PL excitation spectrum of the  $\text{Al}_2\text{O}_3:\text{Mg}$  ceramics contains three most intense bands at 290, 315, and 420 nm (Fig. 3a). Excitation at 290 nm causes emission at 767 nm. The emission band with the maximum at 673 nm dominates when the band at 315 nm is excited, while emission at 689 nm dominates when the band at 420 nm is excited. The emission bands at 674–678, 692–694, and 777–779 nm are attributed to the impurity defects caused by  $\text{Mn}^{4+}$  (the  $R$  band),  $\text{Cr}^{3+}$  (the  $R$  band), and  $\text{Ti}^{3+}$  cations, respectively, which are always present in aluminum oxide [15]. The first two emission bands correspond to  ${}^2E \rightarrow {}^4A_2$  transitions, while the third one corresponds to the  ${}^2E \rightarrow {}^2T_2$  transition. Luminescence at 693 and 676 nm was detected in the CPL spectra of the ceramics under study. The CPL spectrum contained no emission band at 767 nm. It should be mentioned that reduction of impurity concentration decreases the intensity of this band. At impurity concentration of 1 wt %, this band is not detected in the PL spectrum. Let us mention that this band is excited at 4.15 eV, which corresponds to excitation of aggregate  $F_2^{2+}$  or the impurity centers of  $\text{Mg}^{2+}$  cations. As opposed to the band at 767 nm, the emission intensity at 673 and 689 nm decreases with increasing magnesium concentration. Luminescence quenching at 673 nm is more significant than at 689 nm. Thus, luminescence intensity at 689 nm decreased 2.5-fold after dopant concentration was increased by almost three orders of magnitude (from 0.01 to 6.85 wt %); luminescence intensity at 673 nm decreased more than 100-fold (Fig. 4).

Figure 5 shows the TL curves of the studied ceramics sintered at different temperatures at magnesium concentrations of 0.01 and 6.85 wt %. Three peaks at

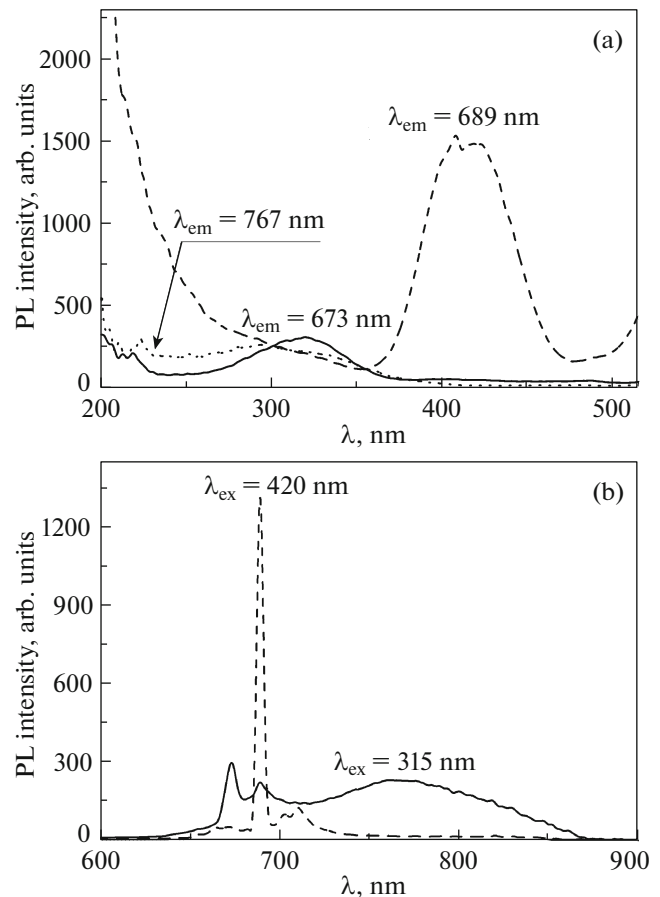


**Fig. 3.** PL excitation (a) and emission (b) spectra of the ceramics with magnesium concentration of 6.85 wt % sintered at  $1700^\circ\text{C}$ .

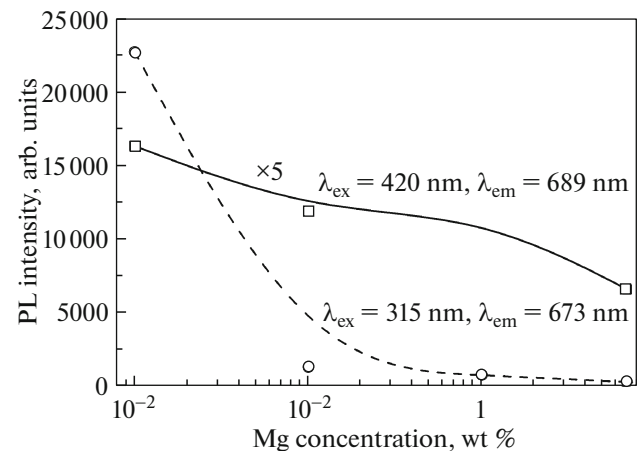


**Fig. 4.** PL intensity as a function of dopant concentration for different emission and excitation bands.

380, 460, and 615 K can be singled out in the diagrams for both concentrations. It is known from the literature data [27] that luminescence of the intrinsic centers of

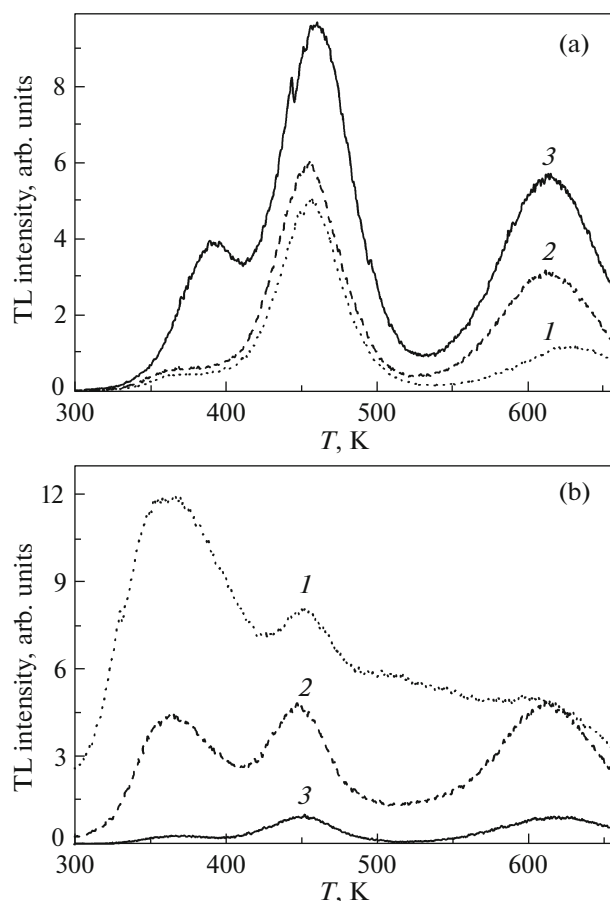


**Fig. 5.** TL curves of the studied ceramics with magnesium concentration of 0.01 wt % (a) and 6.85 wt % (b) at varied sintering temperatures: (1) 1500°C; (2) 1600°C; and (3) 1700°C.

alumina is detected at 450–470 K, while luminescence of the impurity centers of chromium is detected at 620–640 K. The sintering temperature for different dopant concentrations has different effects of TL intensity of all the recorded peaks. Thus, at dopant concentration of 0.01 wt %, a rise in sintering temperature increases luminescence intensity, while the peak from the intrinsic luminescence centers of alumina ceramics is the most intense peak at 460 K. At high magnesium concentration (6.85 wt %), an increase in sintering temperature has a negative impact on luminescence intensity, and luminescence quenching is observed. The peak at 380 K is the dominant peak for this dopant concentration at sintering temperature of 1500°C. The intensities of all TL peaks are comparable at 1600°C, and the high-temperature peaks are most intense ones at 1700°C. In this connection, the low-temperature peak at 380 K can be attributed both to magnesium impurity and to the more complex centers that were formed in the ceramics under study.

Luminescence quenching of the intrinsic centers of alumina and the impurity centers of chromium is

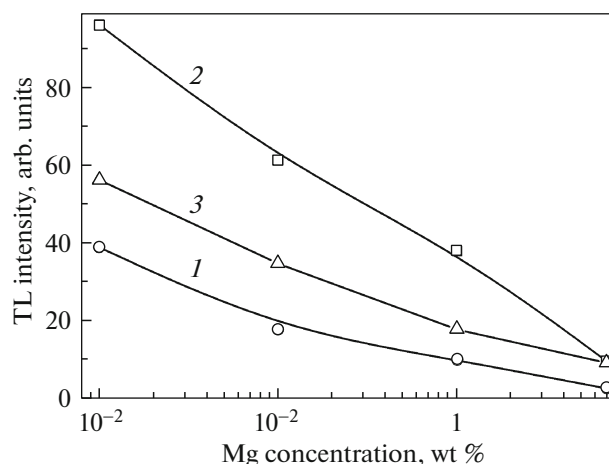


**Fig. 6.** TL intensity as a function of dopant concentration for different PL peaks: (1) 380; (2) 450; and (3) 615 K.

observed in the TL curves and the PCL spectra as concentration of magnesium ions increases (Fig. 6). Meanwhile, a rise in concentration of magnesium ions increases PCL intensity at 520 nm and reduces TL intensity at 390 K. This phenomenon can be responsible for the complex structural state of this defect.

## CONCLUSIONS

Hence, the PCL and PL spectra, as well as the TL curves, were recorded to evaluate the effect of concentration of magnesium ions on luminescence of both the intrinsic centers of alumina ceramics and impurity centers formed during high-temperature sintering under vacuum. The presence of strongly reducing medium during sintering gives rise to a lower concentration of impurity centers of magnesium. It has been demonstrated that the increase in concentration of magnesium ions leads to quenching of the principal luminescence band of alumina (*F* centers). The emission band at 520 nm is recorded at dopant concentrations >1 wt %; its intensity increases with concentration. An analysis of the PL spectra revealed a similar effect. The emission band at 767 nm was found only at high magnesium concentrations; increasing magnesium concentrations resulted in luminescence quenching at the remaining emission bands in the spectrum. The TL curves contain three luminescence peaks with the maxima at 380, 460, and 615 K. The intensity of these peaks decreases with increasing concentration of magnesium ions.

## FUNDING

This work was supported by the Russian Science Foundation (project no. 18-72-10082).

## REFERENCES

1. S. P. Feofilov, A. B. Kulinkin, A. K. Kaveev, N. S. Sokolov, and S. M. Suturin, *Opt. Mater.* **83**, 43 (2018).
2. I. N. Ogorodnikov, M. D. Petrenko, and V. Yu. Ivanov, *Phys. Solid State* **60**, 134 (2018).
3. K. W. Park, H. S. Lim, S. W. Park, G. Deressa, and J. S. Kim, *Chem. Phys. Lett.* **636**, 141 (2015).
4. S. V. Nikiforov and V. S. Kortov, *Phys. Solid State* **59**, 1717 (2017).
5. M. Oja, E. Töldsepp, E. Feldbach, H. Mägi, S. Omelkov, and M. Kirm, *Rad. Meas.* **90**, 75 (2016).
6. S. V. Gorbunov, A. F. Zatsepin, V. A. Pustovarov, S. O. Cholakh, and V. Yu. Yakovlev, *Phys. Solid State* **47**, 733 (2005).
7. D. Liu, *Ceram. Int.* **39**, 4765 (2013).
8. I. V. Gasenkova, N. I. Mukhurov, S. P. Zhvavyi, E. E. Kolesnik, and A. P. Stupak, *J. Lumin.* **185**, 298 (2017).
9. Q. Liu, Q. Yang, G. Zhao, and S. Lu, *J. Alloys Compd.* **582**, 754 (2014).
10. N. Rakov and G. S. Maciel, *J. Lumin.* **127**, 703 (2007).
11. K. Drdlíková, R. Klement, D. Drdláka, T. Spusta, D. Galusekb, and K. Maca, *J. Eur. Ceram. Soc.* **37**, 2695 (2017).
12. Y. Gui, Q. Yang, Y. Shao, and Y. Yuan, *J. Lumin.* **184**, 232 (2017).
13. E. H. Penilla, Y. Kodera, and J. E. Garay, *Adv. Funct. Mater.* **23**, 6036 (2013).
14. B. D. Evans, G. J. Pogatshnik, and Y. Chen, *Nucl. Instrum. Methods Phys. Res., Sect. B* **91**, 258 (1994).
15. A. I. Kostyukov, A. V. Zhuzhgov, V. V. Kaichev, A. A. Rastorguev, and V. N. Snytnikov, *Opt. Mater.* **75**, 757 (2018).
16. N. M. Trindade and L. G. Jacobsohn, *J. Lumin.* **204**, 598 (2018).
17. J. M. Kalita and M. L. Chithambo, *J. Lumin.* **182**, 177 (2017).
18. D. Valiev, O. Khasanov, E. Dvilis, S. Stepanov, E. Polisadova, and V. Paygin, *Ceram. Int.* **44**, 20768 (2018).
19. M. G. Brik, J. Papan, D. J. Jovanović, and M. D. Dramićanin, *J. Lumin.* **177**, 145 (2016).
20. B. S. Choi, O. G. Jeong, J. C. Park, J. W. Kim, S. J. Lee, J. H. Ryu, J. I. Lee, and H. Cho, *J. Ceram. Proc. Res.* **17**, 778 (2016).
21. S. S. Raj, S. K. Gupta, V. Grover, K. P. Muthe, V. Natarajan, and A. K. Tyagi, *J. Mol. Struct.* **1089**, 81 (2015).
22. S. V. Zvonarev, V. S. Kortov, A. V. Chikin, and P. P. Sannikov, in *Physics, Technologies and Innovation (PTI-2016)*, Ed. by V. A. Volkovich, *AIP Conf. Proc.* **1767**, 020025 (2016).
23. A. B. Kulinkin, S. P. Feofilov, and R. I. Zakharchenya, *Phys. Solid State* **42**, 857 (2000).
24. S. Sanyal and M. S. Akselrod, *J. Appl. Phys.* **98**, 033518 (2005).
25. V. Kortov, A. Kiryakov, S. Nikiforov, D. Ananchenko, and S. Zvonarev, *Vacuum* **143**, 433 (2017).
26. V. Kortov, S. Zvonarev, A. Kiryakov, and D. Ananchenko, *Mater. Chem. Phys.* **170**, 168 (2016).
27. M. S. Akselrod, V. S. Kortov, D. I. Kravetsky, and V. I. Gotlib, *Rad. Prot. Dosim.* **32**, 15 (1990).

*Translated by D. Terpilovskaya*